Role of depolarization in the polarization reversal in ferroelectrics

M. Kingsland,[*] Z. G. Fthenakis,[*] and I. Ponomareva
Department of Physics, University of South Florida, Tampa, Florida 33620, USA

Atomistic first-principles-based simulations are used to investigate polarization reversal in ferroelectrics in both the intrinsic and extrinsic regimes in order to determine the origin of nearly an order of magnitude difference in the coercive field predicted theoretically and observed in experiments. We find that the residual depolarizing field that is routinely ignored from considerations is responsible for the drastic reduction of the coercive field. The depolarizing field stabilizes a polydomain phase which allows for counterintuitive cooperation with the applied field to achieve polarization reversal in an energy-efficient way. Contrary to the common belief that low coercive field necessitates polarization reversal via domains formation and propagation, we predict that the same fields could be achieved if the residual depolarizing field is taken into account. An efficient way to incorporate such depolarizing field in any type of atomistic simulations is proposed, which is expected to resolve the longstanding issue of overestimation of fields in simulations of ferroelectrics.

I. INTRODUCTION

Ferroelectrics are the materials that develop spontaneous polarization that is reversible by the application of external electric field. The field at which the polarization reverses its sign is termed the coercive field, E_c, and is an important characteristic of a ferroelectric as it quantifies the easiness of polarization reversal. Technologically, the polarization reversal is in the heart of the ferroelectric memories. Experimentally, the coercive field depends on the electric-field frequency, material, sample type (ceramics or single crystal), grain size, sample thickness, temperature, orientation, and others. For example, for a prototypical ferroelectric PbTiO$_3$, E_c is in the range 0.053–0.250 MV/cm [1,2]. Not surprising, the subject of polarization reversal has remained the focus of attention for decades [3–8]. The polarization reversal can occur via nucleation of the domain with antiparallel polarization direction. The energy change for such nucleation is $\Delta W = \sigma A + W_E - PEV$, where the first term gives the energy of the domain wall, the second term is the depolarizing energy, and the last term is the energy due to applied electric field [9]; P, E, and V are the polarization, applied electric field and the volume of the nucleus, respectively. The rate of domain nucleation is proportional to $e^{-\Delta W/k_B T}$. The probability of nucleation by thermal fluctuations is extremely small since ΔW is about $10^8 \, k_B T$, primarily from the depolarizing energy. It is reasonable to expect that at the crystal surfaces, inhomogeneities or existing domains ΔW can be considerably smaller [9,10]. As a result, the polarization reversal via domains is expected to occur in the extrinsic regime associated with the presence of defects. As the electric field increases, ΔW decreases and, at sufficiently high field, a homogeneous polarization reversal can occur. It can be viewed as nearly simultaneous nucleation

of many tiny domains with antiparallel polarization direction, promoted by the increase in entropy. The polarization reversal in the absence of defects occurs in the intrinsic regime. Such homogeneous switching has been reported [11,12]. The intrinsic polarization reversal has much larger E_c [10]. For example, for 90° polarization switching without domain-wall motion in a BaTiO$_3$ crystal, the coercive field is 500 V/mm, which is to be compared with 80 V/mm via 90° domain-wall motion. The fundamental question is how the polarization reversal evolves from its intrinsic limit associated with high E_c to the extrinsic one associated with drastically lower E_c. What type of defects or their energetic contribution is responsible for such a crossover? Does the extrinsic polarization reversal require domains, and does the intrinsic one exclude them?

Experimentally, these questions are challenging to address as the extrinsic contributions are unavoidable and rarely can be quantified. Computationally and theoretically, on the other hand, the challenge is in incorporating realistic extrinsic contributions in the models. Indeed, the majority of simulations study defect-free, surfaceless samples. Not surprising, the E_c in models and computations often overestimates the experimental ones [13–16]. This brings a methodological question of whether it is possible to introduce a universal yet realistic type of defect to simulations which is capable of bringing the computational E_c in agreement with experiment. Recently, an analytical first-principles-based model has been developed to accurately predict the ferroelectric hysteresis loops at realistic sizes and timescales [17]. The model, however, is limited to domain-driven polarization reversal. Another atomistic study examined the dynamics of preexistent domains in BaTiO$_3$ [18]. An atomistic study on BiFeO$_3$ found an inhomogeneous switching mechanism in tetragonal phases and a homogeneous switching for the rhombohedral phases [16]. Previously, domain-driven polarization reversal was predicted in Pb(Ti$_{1-x}$, Zr$_x$)O$_3$ nanowires under lower electric field, while

---

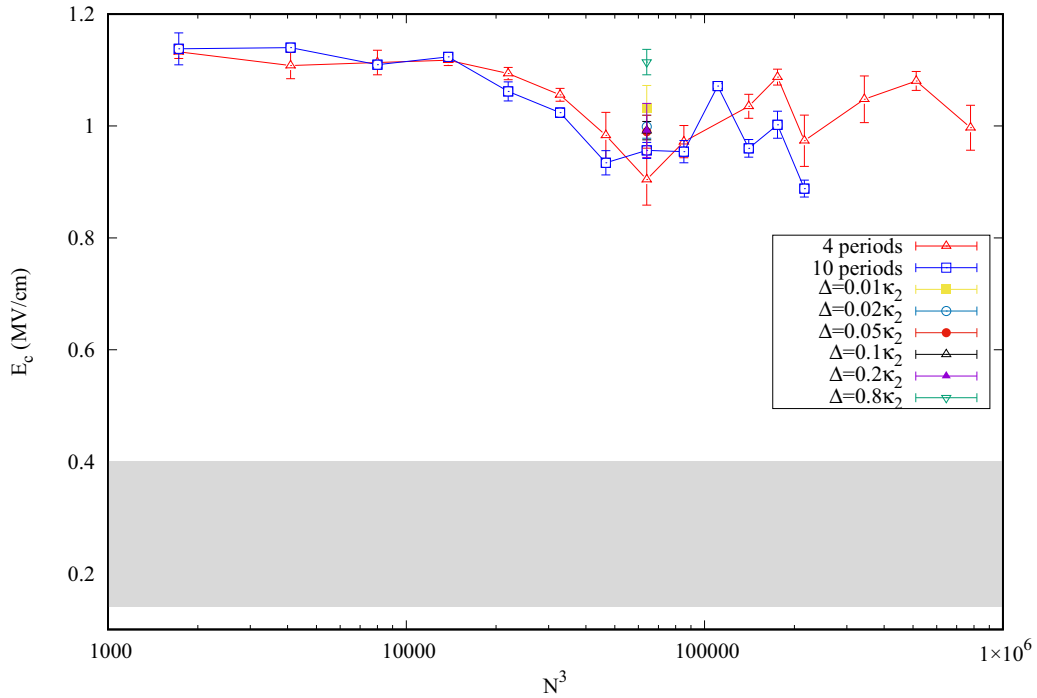[*]These authors contributed equally to this work.

FIG. 1. Dependence of the coercive field on the supercell size. The shaded area indicates the range of experimental coercive fields from the literature [1,2,25].

homogeneous polarization reversal was predicted under larger fields [19]. Motivated to address the important questions about polarization reversal, we carry out first-principles-based molecular dynamics (MD) simulations on bulk PbTiO$_3$.

II. METHODOLOGY

The interatomic interactions are modeled by the first-principles-based effective Hamiltonian of Ref. [20] that provides a simultaneously accurate description of both the static and dynamical properties of this material. In particular, it predicts the transition from a paraelectric to ferroelectric phase at 625 K, which somewhat underestimates the experimental value of 760 K [21–23]. It accurately describes soft-mode frequencies in a wide temperature range [20]. The degrees of freedom for the Hamiltonian include local modes $\mathbf{u}_i$, which are proportional to the dipole moment in the unit cell, and strain variables tensors η_i (in Voigt notations), which are responsible for the mechanical deformations of a unit cell. The energy of the Hamiltonian is [20]

$$
\begin{aligned}
E^{\text{tot}} = {} & E^{\text{FE}}(\{\mathbf{u}_i\}) + E^{\text{elas}}(\{\eta_i\}) \\
& + E^{\text{FE-elas}}(\{\mathbf{u}_i, \eta_i\}) + E^{\text{elec}}(\{\mathbf{u}_i\}),
\end{aligned} \tag{1}
$$

where E^{FE} is the energy associated with the ferroelectric local modes and includes contributions from the dipole-dipole interactions, short-range interactions, and on-site self-energy. The second term E^{elas} is the elastic energy associated with the unit-cell deformations. $E^{\text{FE-elas}}$ is the energy contribution due to the interactions between the ferroelectric local modes and the strain. The last term gives the interaction energy between the local modes and an external electric field. Periodic boundary conditions are applied along all three Cartesian directions

to simulate bulk samples. Calculations were carried out at constant temperature of 300 K by utilizing the Evans-Hoover thermostat [24] with a MD step of 1.0 fs.

III. RESULTS AND DISCUSSION

We begin with the investigation of the polarization reversal in PbTiO$_3$ in the intrinsic regime that is in defect-free bulk samples.

Intrinsic regime: Supercell size effect. We first assess the dependence of E_c on the simulation's supercell size. The hypothesis is that larger supercells allow for larger fluctuations from the average values, which, in principle, could lead to the formation of the critical size nucleus. The supercell sizes of $N \times N \times N$ unit cells of cubic perovskites were considered with N in the range of 12 to 92 with the step of 4 unit cells. For sizes up to $N = 60$, we simulated 10 periods of electric field whose frequency was 10 GHz, while for larger sizes, we simulated only 4 periods due to computational limitations. Figure 1 shows our data for $E_c(N^3)$ along with the range of experimental data for PbTiO$_3$ and lead titanate zirconate, PZT. The data predict no size dependence within the size range investigated. The average value of E_c is 1.1 ± 0.01 MV/cm, which significantly overestimates the experimental values of 0.14–0.30 MV/cm in PbTiO$_3$ and PZT [1,2,25].

Intrinsic regime: Electric-field frequency. The E_c exhibits dependence on frequency. To investigate this dependence, we applied an ac electric field with the frequency in the range of 0.01 to 10 GHz to the simulation supercell of $40 \times 40 \times 40$ unit cells. The frequencies higher than 10 GHz will already overlap with the intrinsic soft-mode dynamics range, while frequencies below 0.01 GHz are computationally prohibitive. These data are given by the green diamonds in Fig. 4(c).
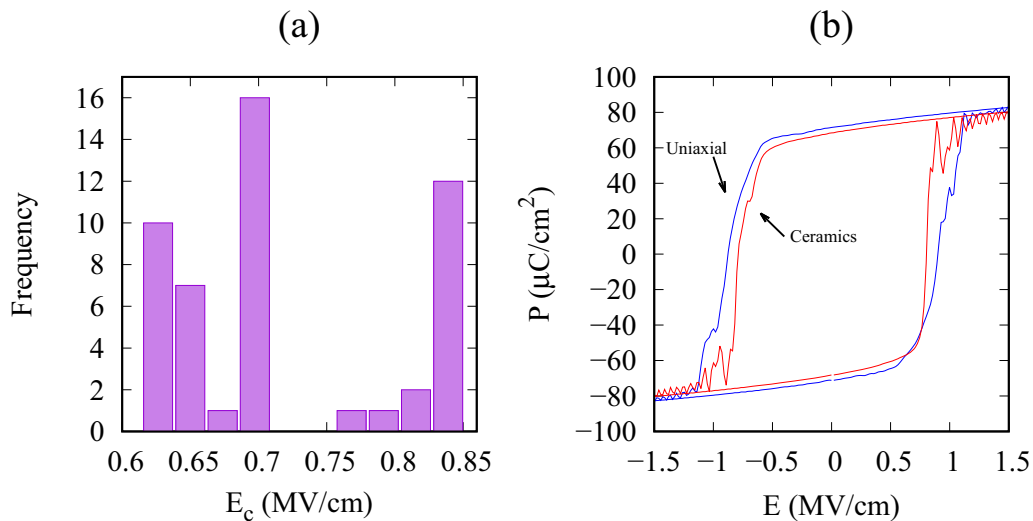
FIG. 2. (a) Distribution of E_c obtained for different directions of the applied electric field and (b) comparison between the hysteresis loops simulating a ceramic and single-crystalline sample (uniaxial). In the latter one, the field is applied along the polar direction.

Within the investigated range of frequencies, the intrinsic E_c shows rather weak frequency dependence which extrapolates to 0.97 MV/cm at zero Hz and significantly overestimates the experimental values. On the basis of investigations in the intrinsic regime, we conclude that the intrinsic E_c in PbTiO$_3$ is around 1 MV/cm. Next, we turn to the investigation of the extrinsic regime.

Extrinsic regime: Electric-field direction. Many ferroelectric samples are grown in the form of polycrystalline ceramics with small crystallites being randomly oriented crystallographically [26]. The polarization reversal in this case should take into account the domain reorientation in each grain and the polycrystalline state as a complex of randomly oriented crystals. This, for example, results in nearly 83% decrease in spontaneous polarization in ceramics as compared to single crystals [26]. As a result, E_c is also expected to be affected by the state of the sample. In order to model a polycrystalline sample, we subjected the simulated supercell of $40 \times 40 \times 40$ to an electric field applied along different crystallographic directions. In particular, 50 directions of the applied field uniformly sampled on the surface of a unit sphere were selected. The frequency of the field was 10 GHz. The distribution of E_c obtained from the 50 simulations is given in Fig. 2(a), where E_c ranges from 0.60 to 0.84 MV/cm, as compared to the average value of 0.90 ± 0.05 MV/cm for this supercell under the electric field applied along the polar direction. To model the hysteresis loop of ceramics, we averaged the loops obtained for the 50 different field directions. Figure 2(b) gives this data in comparison with single-crystalline computational data. We find the decrease in spontaneous polarization of 2.7% and in E_c of only 10.9%. Surprisingly, we find that while E_c indeed decreases in polycrystalline samples, it still significantly overestimates the experimental values. Therefore, the polycrystallinity of the sample cannot account for the overestimation of the E_c in computations.

Extrinsic regime: Epitaxial strain. The next extrinsic effect to be considered is the epitaxial strain η that arises from the lattice mismatch between the ferroelectric film and the substrate. We simulated η in the range $[-0.95 : 0.95]$% applied in the [001] plane, which is perpendicular to the direction of the applied electric field. We modeled four periods of the electric field whose frequency was 10 GHz. The simulation supercell size was $40 \times 40 \times 40$. A few representative loops are given in Fig. 3(a). Epitaxial strain was found to have a pronounced effect on the E_c. Compressive strain broadens the loops, while tensile strain makes them slimmer. We found that for tensile strains of magnitude >0.65%, no spontaneous polarization appears along the direction of the field. The dependence $E_c(\eta)$ is given in Fig. 3(b) and can be fitted with a linear function, $-1.2\eta + 0.8$ MV/cm. We conclude that the extrinsic effect of epitaxial strain could account for the reduction of E_c with respect to its intrinsic value in samples under tensile strain. On the other hand, for the samples which experience compressive epitaxial stain, the enhancement of E_c with respect to the intrinsic value is expected. However, to the best of our knowledge, this has not been observed experimentally.

Extrinsic regime: Microstructure inhomogeneity. We next hypothesize that variations in the microstructure that are inevitable in experiments give rise to the local variations in the ferroelectric strength. In simulations, such variations are expected to promote a more inhomogeneous distribution among the local dipoles and potentially create regions that could serve as nucleation sites. To model this, we introduced local variation in the κ_2 on-site interaction parameter of the effective Hamiltonian that controls the depth of the local ferroelectric well. Technically, the values of κ_2 for each site were picked randomly from a normal Gaussian distribution. The width of the distribution, Δ, was 1%, 2%, 5%, 10%, 20%, or 80% of the first-principles value of κ_2. These simulations were carried out on a $40 \times 40 \times 40$ supercell subjected to the electric field of frequency 10 GHz. We found no trend in the dependence of E_c on the local variations of the ferroelectric strength (see Fig. 1).

Extrinsic regime: Depolarization. The last extrinsic effect that we investigate is the effect of the residual depolarizing
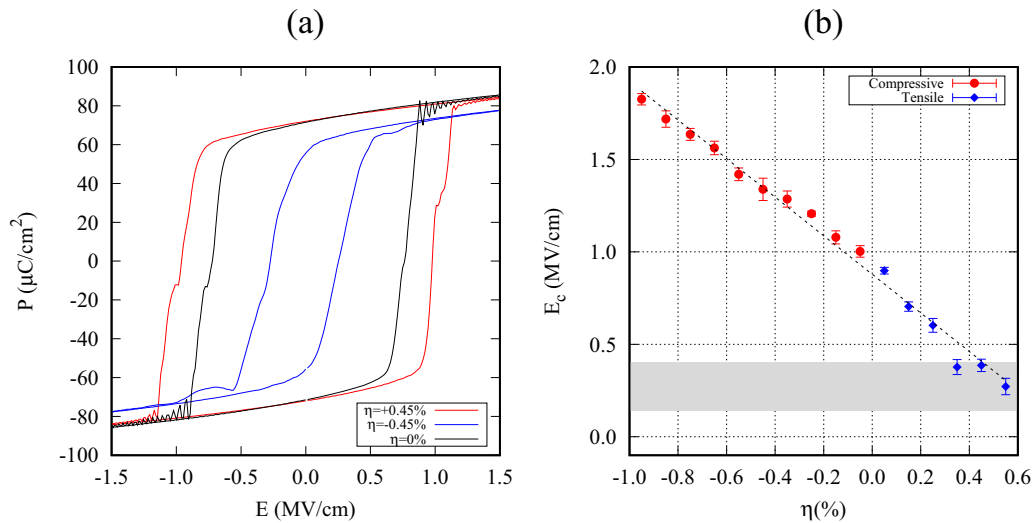
FIG. 3. (a) Representative hysteresis loops for different percentage of epitaxial strain and (b) the dependence of E_c on the epitaxial strain. The shaded area indicates the range of experimental coercive fields from the literature [1,2,25].

field that is always present in real samples due to their finite sizes as well as the presence of inhomogeneities. The depolarizing field is responsible for the multidomain phase of the grown ferroelectric samples. During poling of macroscopic samples in experiments, the free carriers are mostly able to screen this depolarizing field. The screening carriers could be internal (vacancies within the sample, for example) or external (from electrodes) [27]. As the thickness of the sample decreases and the amount of the internal screening charge decreases, the dead layer becomes crucial, while the depolarizing field remains mostly constant (at least under the assumptions of macroscopic electrostatics). Ultrathin films tend to remain in nanodomain phases [28]. Effects of the residual depolarizing field are commonly ignored in the polarization reversal studies as it is assumed that the free charge from the electrodes screen such a field entirely. We hypothesize that the residual depolarizing field due to imperfect screening of polarization discontinuities could have a significant effect on the polarization reversal and E_c. For example, on the basis of statistical switching kinetics modeling, it was predicted that the switching time in polycrystalline thin films goes to infinity when the applied electric field is less than the maximum depolarizing field in the sample [29]. In the followup study of a two-dimensional case, it was shown that switching starts earlier supported by the depolarization fields formed in the initial opposite polarization state [30].

To introduce a universal-type defect in simulations that leads to the onset of the depolarizing field, we incorporate an extended nonpolarizable (or weakly polarizable) region in the supercell. Technically, this could be achieved by introducing a vacuum layer in the supercell, where the electric dipoles are missing [see Fig. 4(a), type-I defect]. The hysteresis loop associated with such a defected supercell is given in Fig. 4. Surprisingly, we find a double-loop structure similar to the one for antiferroelectrics. At zero field, the multidomain phase is stable due to the presence of strong depolarizing field, while the polar phase can be induced by the application of electric field comparable in magnitude with the intrinsic E_c of

the material. Note that the double-loop structures have been observed in some ferroelectrics experimentally [9,31,32]. In order to partially screen the depolarizing field, we reduce the size of the defected region, as schematically shown in Fig. 4(a) (defect type II). In particular, we introduced an island that connects the ferroelectric regions in the periodic images of the supercell. As the size of the island increases, the $P(E)$ response regains its single-loop structure that indicates that the depolarizing field has decreased enough to allow for the supercell to be poled. An example of the response of the film with 1.54% defect content is given in Fig. 4(b) and compared with the response of the defect-free supercell and experimental data for PbTiO$_3$ from the literature. We found that the depolarizing field has a drastic effect on the E_c, reducing it by more than a half and bringing it in agreement with experiment. The values of saturation and remnant polarization are only decreased by 8.68% and 14.9%, respectively. We have also considered another type of extended defect [type III in Fig. 4(a)]. Simulations were carried out at frequencies of 0.5, 1, and 10 GHz.

In all cases, we only focus on the data that predict a single loop as this is expected in realistic simulations of the residual depolarizing field. The E_c obtained from these simulations is given as a function of frequency in Fig. 4(c). The depolarizing field has a profound effect on the E_c at all frequencies investigated. For comparison, we also carried out simulations for the limiting defect size of one unit cell, with the defects distributed randomly in the supercell [type IV in Fig. 4(a)]. Some of those data are added to Fig. 4(c). Note that the extended type of defects (types II and III) is an efficient way to incorporate a residual depolarizing field in simulations and does not need to be correlated with the actual structure of the sample. In fact, any type of extended defects that allows for poling is equally suitable. For example, in Ref. [33], other shapes of extended defects were investigated and found to have a similar effect on E_c.

We can see that even the tiniest nonpolar defects have a significant effect on the E_c [34], but not as strong as the
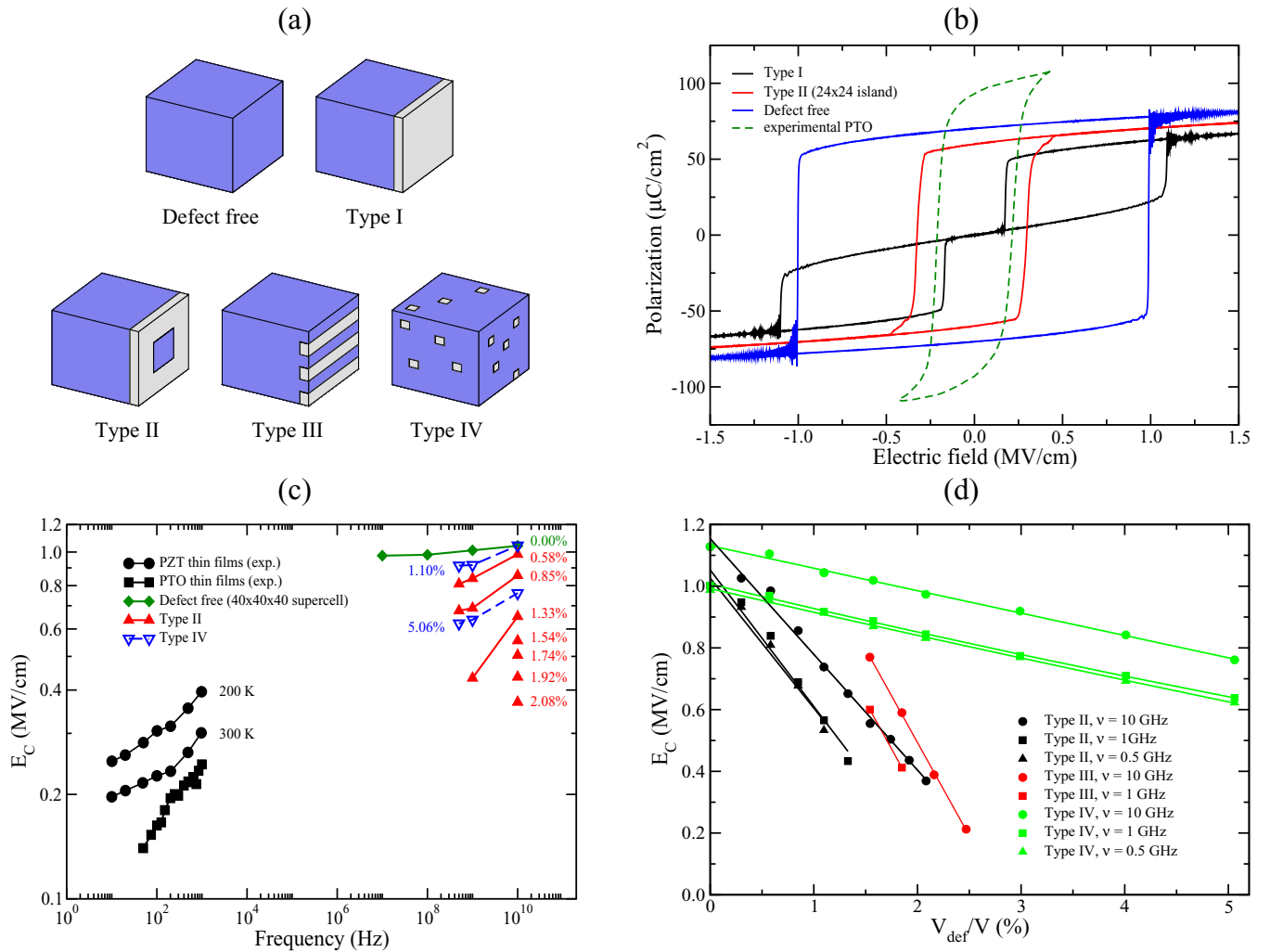
FIG. 4. The effect of the residual depolarizing field on the E_c. (a) Schematic representation of different types of defects; (b) some representative computational hysteresis loops obtained for a $36 \times 36 \times 36$ supercell under 1 GHz electric field (solid lines) and experimental one for epitaxial $PbTiO_3$ film measured at 10 kHz [1]; (c) the dependence of E_c on the frequency of applied field from computations and experiments of Refs. [2] (black solid squares) and [25] (black solid circles); (d) the dependence of E_c on the defected volume ratio V_{def}/V, for different types of defects; simulation supercell size is $36 \times 36 \times 36$.

extended types. Figure 4(d) shows the dependence of E_c on the relative volume of defects of different types, V_{def}/V. The slope of $E_c(V_{\mathrm{def}}/V)$ significantly depends on the type of defects. The smallest slope is for the type-IV defects, which we attribute to the smallest depolarizing field in this case. Extended types of defects (types II and III) exhibit significantly larger slopes and a transition into a double-loop response at the critical defect volume associated with zero value of E_c. No such transition for defect type IV has been found. In this case, the zero value of E_c occurs at extremely high $V_{\mathrm{def}}/V = 25\%$ at which the supercell exhibits paraelectric behavior.

Our most critical finding is that the residual depolarizing field in ferroelectric samples introduces the competition between monodomain and multidomain phases, which significantly affects the polarization reversal and associated E_c. At the basic modeling level, such a field makes a positive contribution, $-E_{\mathrm{dep}}PV \propto \alpha P^2 V$, to the free energy of the ferroelectric and, therefore, destabilizes the ferroelectric phase. When the critical nucleus of antiparallel polarization

of volume V_n is formed, roughly twice of that volume has zero net polarization and no longer contributes the destabilizing depolarizing energy $-E_{\mathrm{dep}}P2V_n \propto \alpha P^2 2V_n$ to the free energy. Alternatively, this could be considered as an additional stabilizing energy for the critical nucleus. Because E_{dep} could reach very large values, a significant reduction in the ΔW is expected. What is rather counterintuitive is that the depolarization actually cooperates with the applied field to reverse the polarization. The extended defects simulate a realistic scenario when the depolarizing field originates from the discontinuity in polarization at the surface of the sample, grain boundaries, or other inhomogeneities. Interestingly, residual stresses have also been found to affect the kinetics of polarization reversal in polycrystalline samples [35]. It should be noted that sample conductivity increases with temperature so that the contribution of the depolarization will diminish significantly (or even disappear all together) as the sample is heated to the Curie point [9]. Therefore, we do not expect the depolarization effects to significantly affect the Curie temperature.

We also have looked into the mechanism of polarization reversal in some of our calculations. In some cases, we detected the formation of domains that are relatively large in size. However, the appearance of the domains during the polarization reversal seems to be rather random and infrequent under the simulated conditions. We propose that the appearance of domains that are well defined and relatively large in size is driven by the minimization of the domain-wall area, but makes a relatively small contribution to energy as compared to the effects of the residual depolarizing field or ferroelasticity. This is based on the rather infrequent appearance of domain-driven polarization reversal in our simulation. Lower electric-field frequencies (such as typical experimental frequencies) allow for larger fluctuations, allowing for the system to follow the lowest free-energy path associated with domain formation. At higher frequencies (like the ones simulated here), the fluctuations sufficient to nucleate a domain do not occur often, which explains the infrequent appearance of domains during polarization reversal. Furthermore, domain growth takes time which may be longer than the simulation time. Experimentally, it was found that the domain size decreases as the pulse width of the electric field decreases, and saturates at about 20 nm in radius for pulse width below 10^{-5} s [36]. We, therefore, expect that as the frequency of the electric field decreases, the domain-driven polarization reversal will occur more and more frequently, eventually becoming the main polarization reversal mechanism.

We also have repeated some of the simulations in the presence of the residual depolarizing field for another ferroelectric, BaTiO$_3$, using the interatomic potential of Ref. [37]. Overall, we found very similar behavior. Most importantly, the residual depolarizing field reduced E_c by half or more.

IV. CONCLUSIONS

In summary, we investigated the polarization reversal and associated E_c in a prototypical ferroelectric PbTiO$_3$ in both intrinsic and extrinsic regimes. We found that the intrinsic E_c at frequencies above 0.1 GHz is about 1 MV/cm, which is more than twice the experimental value. In the extrinsic regime, we found that the E_c for ceramics is slightly lower than the one for single-crystalline samples, but the reduction is too small to account for the discrepancy with the experimental data. The epitaxial strain was found to have a profound effect on E_c. In particular, E_c is reduced under epitaxial tension and increased under epitaxial compression. However, given that the predicted enhancement of E_c with respect to intrinsic values in compressed samples has not been reported experimentally to the best of our knowledge, it is unlikely that the epitaxial strain is primarily responsible for the reduced E_c in the extrinsic regime. The effect of microstructure variation was found to have an insignificant effect on E_c. On the other hand, the residual depolarizing field that is routinely ignored in polarization reversal studies was found to have a critical effect on the polarization reversal and the associated E_c. In particular, in PbTiO$_3$ and BaTiO$_3$, the field introduces a strong competition between the monodomain and polydomain phases, which reduces E_c by more than half and brings it within the experimental range of values. A basic way to account for such residual depolarizing field in any type of atomistic simulations is proposed. We believe that our study advances the fundamental understanding of polarization reversal in ferroelectrics and will stimulate further research in this direction.

[1] W.-H. Kim, S. M. Yoon, and J. Y. Son, Mater. Lett. **124**, 47 (2014).

[2] A. Iljinas, L. Marcinauskas, and V. Stankus, Appl. Surf. Sci. **381**, 6 (2016).

[3] W. J. Merz, Phys. Rev. **95**, 690 (1954).

[4] H. L. Stadler, J. Appl. Phys. **29**, 1485 (1958).

[5] P. Gao, J. Britson, J. R. Jokisaari, C. T. Nelson, S.-H. Baek, Y. Wang, C.-B. Eom, L.-Q. Chen, and X. Pan, Nat. Commun. **4**, 2791 (2013).

[6] R. Xu, S. Liu, I. Grinberg, J. Karthik, A. R. Damodaran, A. M. Rappe, and L. W. Martin, Nat. Mater. **14**, 79 (2015).

[7] R. Xu, R. Gao, S. E. Reyes-Lillo, S. Saremi, Y. Dong, H. Lu, Z. Chen, X. Lu, Y. Qi, S.-L. Hsu, A. R. Damodaran, H. Zhou, J. B. Neaton, and L. W. Martin, ACS Nano **12**, 4736 (2018).

[8] Z. Chen, L. Hong, F. Wang, S. P. Ringer, L.-Q. Chen, H. Luo, and X. Liao, Phys. Rev. Lett. **118**, 017601 (2017).

[9] M. Lines and A. Glass, *Principles and Applications of Ferroelectrics and Related Materials* (Clarendon Press, Oxford, 1977).

[10] J. F. Scott, Ferroelectrics **503**, 117 (2016).

[11] M. J. Highland, T. T. Fister, M.-I. Richard, D. D. Fong, P. H. Fuoss, C. Thompson, J. A. Eastman, S. K. Streiffer, and G. B. Stephenson, Phys. Rev. Lett. **105**, 167601 (2010).

[12] Y. W. Li, J. F. Scott, D. N. Fang, and F. X. Li, Appl. Phys. Lett. **103**, 232901 (2013).

[13] B. K. Mani, C.-M. Chang, S. Lisenkov, and I. Ponomareva, Phys. Rev. Lett. **115**, 097601 (2015).

[14] B. Xu, C. Paillard, B. Dkhil, and L. Bellaiche, Phys. Rev. B **94**, 140101(R) (2016).

[15] B. Luo, X. Wang, E. Tian, L. Wu, and L. Li, J. Appl. Phys. **120**, 074106 (2016).

[16] B. Xu, V. Garcia, S. Fusil, M. Bibes, and L. Bellaiche, Phys. Rev. B **95**, 104104 (2017).

[17] S. Liu, I. Grinberg, and A. M. Rappe, Nature (London) **534**, 360 (2016).

[18] V. Boddu, F. Endres, and P. Steinmann, Sci. Rep. **7**, 806 (2017).

[19] K. McCash, A. Srikanth, and I. Ponomareva, Phys. Rev. B **86**, 214108 (2012).

[20] B. K. Mani, C.-M. Chang, and I. Ponomareva, Phys. Rev. B **88**, 064306 (2013).

[21] J. Remeika and A. Glass, Mat. Res. Bull. **5**, 37 (1970).

[22] G. Shirane, J. D. Axe, J. Harada, and J. P. Remeika, Phys. Rev. B **2**, 155 (1970).

[23] G. Burns, Phys. Rev. Lett. **37**, 229 (1976).

[24] D. Rapaport, *The Art of Molecular Dynamics Simulation* (Cambridge University Press, Cambridge, 1997).

[25] S. M. Yang, J. Y. Jo, T. H. Kim, J.-G. Yoon, T. K. Song, H. N. Lee, Z. Marton, S. Park, Y. Jo, and T. W. Noh, Phys. Rev. B **82**, 174125 (2010).

[26] K. Uchino, *Ferroelectric Devices* (Marcel Dekker, New York, 2000), Chap. 3.

[27] S. V. Kalinin, Y. Kim, D. D. Fong, and A. N. Morozovska, Rep. Prog. Phys. **81**, 036502 (2018).

[28] D. Fong, G. Stephenson, S. Streiffer, J. Eastman, O. Auciello, P. Fuoss, and C. Thompson, Science **304**, 1650 (2004).

[29] X. J. Lou, J. Phys. Condens. Mat. **21**, 012207 (2008).

[30] Y. A. Genenko, J. Wehner, and H. von Seggern, J. Appl. Phys. **114**, 084101 (2013).

[31] T. Rojac, S. Drnovsek, A. Bencan, B. Malic, and D. Damjanovic, Phys. Rev. B **93**, 014102 (2016).

[32] T. Rojac, M. Kosec, B. Budic, N. Setter, and D. Damjanovic, J. Appl. Phys. **108**, 074107 (2010).

[33] P. Fedeli, M. Kamlah, and A. Frangi, Smart Mater. Struct. **28**, 035021 (2019).

[34] Y.-B. Ma, C. Molin, V. V. Shvartsman, S. Gebhardt, D. C. Lupascu, K. Albe, and B.-X. Xu, J. Appl. Phys. **121**, 024103 (2017).

[35] J. E. Daniels, C. Cozzan, S. Ukritnukun, G. Tutuncu, J. Andrieux, J. Glaum, C. Dosch, W. Jo, and J. L. Jones, J. Appl. Phys. **115**, 224104 (2014).

[36] T. Tybell, P. Paruch, T. Giamarchi, and J.-M. Triscone, Phys. Rev. Lett. **89**, 097601 (2002).

[37] R. Herchig, C.-M. Chang, B. K. Mani, and I. Ponomareva, Sci. Rep. **5**, 17294 (2015).